  Bull. Chem. Soc. Jpn., 60, 3367—3372 (1987)

Electrochemical Redox Intercalation of Copper(I) Cation for $Cu_xMo_6S_8$ Superconductor Accompanied with a Reversible Structure Change

Tooru INOUE* and Toshihiro YAMASE
Research Laboratory of Resources Utilization, Tokyo Institute of Technology,
4259 Nagatsuta-cho, Midori-ku, Yokohama 227
(Received November 18, 1986)

Ternary compounds (Chevrel phase compounds) of molybdenum $Cu_xMo_6S_8$ were prepared by sintering mixed powders of MoS_2, Mo, and CuS and employed as electrodes in aqueous solutions. Electrochemical polarization of the electrodes gives rise to intercalation and deintercalation processes of Cu^+, resulting in deformative change in crystal structure of the compounds. The lattice constants of rhombohedral unit cells of the compounds are a_r=6.66 Å, α_r=96°, and V_r=290 Å^3 for the intercalated compound $Cu_4Mo_6S_{7.8}$, and a_r= 6.43 Å, α_r=91.2°, and V_r=267 Å^3 for the fully deintercalated $Mo_6S_{7.8}$. Both the copper(I) composition and the crystal structure of $Cu_xMo_6S_{7.8}$ can be controlled by the electric quantity in electrochemical redox treatment. Structure deformation results from change in electronic distribution of crystal, as well as in charge density of a Mo octahedral cluster, due to electrolysis.

Ternary compounds of molybdenum designated by $M'_xMo_6S_8$ (M' is a metal such as Cu, Pb, Sn, or Fe) have been known as one group of atractive superconducting materials since Chevrel reported relevantly the synthetic methods and basic structures of compounds of this group.[1-5] With respect to critical temperature (T_c) and critical magnetic field (H_c) as characteristic properties of superconductors, $PbMo_6S_8$ possesses the highest T_c (16 K) and H_c (600 kG) values of the members of this group, although Mo_6S_8 which has no metal M' does not show any superconducting property. The T_c value of $Cu_xMo_6S_8$ (x=0—4) changes from 0 to 11 K with increasing value of x. Recent studies have been carried out with their focus on phase digrams, effects of variation in components, and developments of applications such as the construction of secondary batteries and the fabrication of superconducting wires. The crystal structure of the compounds of this group is rhombohedral with a sulfur quasi-cubic cell containing an octahedral molybdenum Mo_6 cluster and metal intercalants. Critical superconducting properties of various Chevrel phase compounds have been reported.[8-10]

Chemical and electrochemical intercalations have been reported for transition metal dichalcogenides (MX_2 where M=Mo, W, Ti, Ta; X=S, Se, Te). Molecules and ions can enter interlayer spaces of these compounds, and it is expected that their electrical conductivities, especially superconductivity, can be enhanced by anisotropic change in electronic charge distribution and crystal structure.[11,12] Chevrel phase compounds may also contain metallic intercalants along the channel space, i.e., a kind of tunnel, of crystal. It is suggested that composition shift of intercalants can affect the superconductive property of compounds. Therefore, study on the relationship between crystal structure and intercalation processes has significance from the standpoint of physical and chemical characterizations and development of applications.

In a previous report, we have described that the redox behavior of $Cu_xMo_6S_{7.8}$ is reversible with respect to both intercalation process and crystal structure change.[13] In this study, redox processes of various copper Chevrel compounds are investigated with particular reference to the deformation of crystal structure in course of redox charge transfer. Anodic and cathodic polarizations of electrode materials lead to reversible redox processes, that is, intercalation and deintercalation of copper(I) cation Cu^+ and result in reversible change in crystal structure. It will be shown that the intercalant composition of $Cu_xMo_6S_{7.8}$ can be controlled by electrolytic charges.

Experimental

Stoichiometric mixtures of powders of CuS, MoS_2, and Mo were ground in acetone. The powder sample was put in a quartz tube, evacuated and dried at ca. 200 °C. The evacuated tube was sealed and set in an electric furnance, and then heated so gradually to 500 °C as to avoid explosion of the tube due to rapid vaporization of the sulfur. The temperature was raised up to 1000 °C, and held there for as long as 100 h for complete equilibration. The sample was then quickly quenched in cold water. A dark gray powder was obtained as a Chevrel phase material. If the sample contained unreacted powder as revealed by powder X-ray diffraction analysis, the above heating procedure was repeated on the sample. The host compound $Mo_6S_{7.8}$, without Cu, was obtained by shaking a 5 M (1 M= 1 mol dm^{-3}) HCl solution with suspended $Cu_2Mo_6S_{7.8}$ in an ultrasonic bath for 1 week. The number of Cu^+ ions which were dissolved into the solution from 1 g of sample powder was ca. 1.25×10^{21} as estimated by a polarographic analysis on the suspended HCl solution. The copper(I) compositions (x) of the other sample compounds were determined, within 3% error, similarly by polarographic analysis on HCl solutions with suspended $Cu_xMo_6S_{7.8}$ powders after shaking. In order to prepare electrodes, the sample powder of 0.3 g was pressed at 300 kg cm^{-2} into a disk with a diameter of

1 cm and a thickness of 1 mm. One face of the disk was connected to a Cu lead wire with conductive silver epoxy resin and covered with insulative epoxy resin.

For electrochemical measurement, three electrodes, i.e., a sample electrode, a Pt counter electrode, and a saturated colomel electrode (SCE), were set in a flask-type glass cell and controlled by a potentiogalvanostat (HD-301, Hokuto Denko Co.). The supporting electrolyte was 0.1 M KNO_3 or 1 M KCl. The intercalant was supplied in the form of CuCl or $Cu(NO_3)_2$. Prior to running electrolyses the aqueous solution was deaerated by N_2 bubbling. In order to detect deintercalated species, the rotating ring-disk electrode (RRDE) method was adopted which used a sample disk of 5 mm diameter and a Pt ring of 7 mm inner 9 mm outer diameter. The measuring technique was described elsewhere.[14,15]

The crystal structures of the samples before and after electrolysis were determined with a powder X-ray diffrometer from Rigaku Denki Co. using Cu $K\alpha$.

Results and Discussion

The behavior of sample electrodes was first investigated in course of redox electrolysis in 0.1 M KNO_3 solutions. Figure 1 shows four cyclic voltammograms of $Cu_xMo_6S_{7.8}$ (x=0, 2, 3, and 4). The oxidation and reduction currents were obtained under anodic and cathodic polarizations. Broad redox waves appear in the potential range [A] between −1.0—0.3 V vs. SCE. These waves have high current densities (>ca. 10 mA cm^{-2} at 0 V vs. SCE) and show good reversibility. The magnitude of redox currents decreases with decrease in the copper composition (x), that is, these currents depend on the composition (x). In the potential range [B] above 0.3 V vs. SCE, another oxidation wave also appears with a remarkably large curent density. When an oxidation current appears at a sample electrode under anodic polarization, a part of solution near the sample electrode turns greenish yellow, with evolution of gas (probably hydrogen) and deposition of Cu on the Pt counter electrode. Although no exact processes occurring on the sample electrode can be determined only from the above potential cycling experiments, it may be estimated that copper cation participates in the redox processes of $Cu_xMo_6S_{7.8}$.

In order to clarify the redox processes for $Cu_xMo_6S_{7.8}$, the rotating ring disk electrode technique was used with application of a $Cu_xMo_6S_{7.8}$ disk and a Pt ring electrode. Figure 2 shows the analytical current-potential curves for the $Cu^{+/2+}$ couple on the Pt ring electrode when oxidation occurs on the $Cu_4Mo_6S_{7.8}$ disk electrode. When oxidation proceeds on the disk at a potential of −0.2 V vs. SCE in the range [A], a large oxidation current from Cu^+ to Cu^{2+} is observed above 0.2 V at the Pt ring electrode. This phenomenon indicates that dissolution of Cu^+ occurs on the sample disk electrode. Then, when an oxidation current appears on the disk at a potential of 0.35 V in the range [B], the oxidation current from Cu^+ to Cu^{2+} decreases and the reduction current from Cu^{2+} to Cu^+ increases on the Pt ring. This phenomenon means that production of Cu^{2+} instead of Cu^+ increases on the disk electrode in this potential

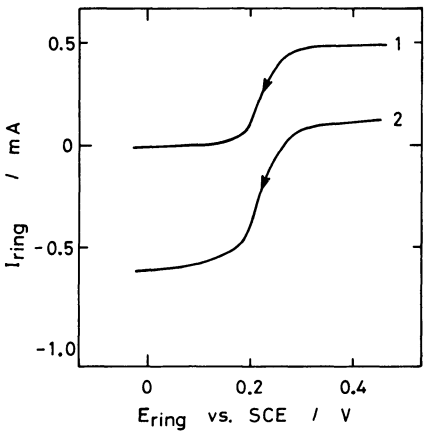

Fig. 2. Current-potential curves at a Pt ring electrode in the course of $Cu_4Mo_6S_{7.8}$ oxidation at a disk at 1000 rpm in 1 M KCl solution. Potentail scan rate is 30 s V^{-1}.
(1) E_{disk}=−0.2 V, I_{disk}=2.5 mA, (2) E_{disk}=0.35 V, I_{disk}=5.2 mA.

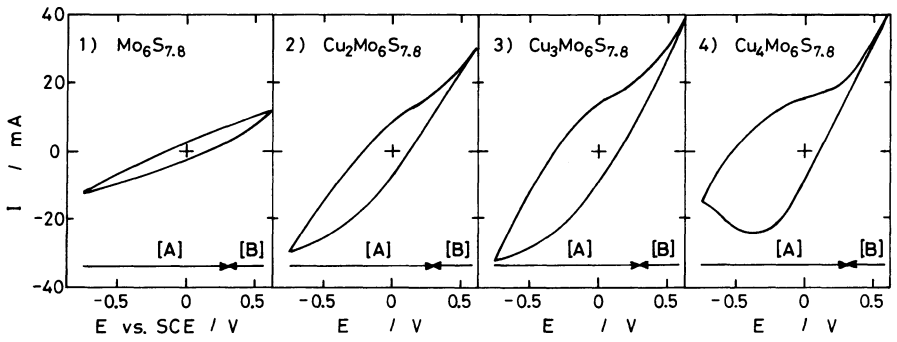

Fig. 1. Cyclic voltammograms of $Cu_xMo_6S_{7.8}$ (x=0, 2, 3, and 4) in 0.1 M KNO_3 solution. Potential scan rate is 30 s V^{-1}.

range, where Cu^{2+} is stabler than Cu^{+} because the standard redox potential of $Cu^{+/2+}$ is ca. 0.3 V vs. SCE in aqueous chloride solution.[14] From these results it is derived that products due to oxidation on $Cu_4Mo_6S_{7.8}$ are Cu^{+} in the potential range [A] and Cu^{2+} in the potential range [B]. The same products were obtained from redox electrolyses on $Cu_2Mo_6S_{7.8}$ and $Cu_3Mo_6S_{7.8}$. For the reduction processes on the $Cu_xMo_6S_{7.8}$ electrodes, similar RRDE techniques were employed on solutions saturated with CuCl. From the RRDE measurements it is derived that the reduction process on $Cu_xMo_6S_{7.8}$ is a consumption process of Cu^{+} in solution. However, no deposition of metallic copper on $Cu_xMo_6S_{7.8}$ disk surface was observed. When we employed Cu^{2+} instead of Cu^{+} in solution for reductive electrolysis, it was recognized through an X-ray diffraction analysis, as mentioned later, that intercalation with Cu^{2+} also occurred on $Cu_xMo_6S_{7.8}$, on the basis of the result of identification that the intercalated sample had the same crystal structure as in the case of Cu^{+}. Therefore, a reduction process of $Cu_xMo_6S_{7.8}$ leads to intercalation of copper(I) cation. From these results, the redox processes can be formulated as;

for oxidation below 0.3 V

$$Cu_xMo_6S_{7.8} \longrightarrow Cu_{x-1}Mo_6S_{7.8} + Cu^{+} + e^{-}, \quad (1)$$

for oxidation above 0.3 V

$$Cu_xMo_6S_{7.8} \longrightarrow Cu_{x-1}Mo_6S_{7.8} + Cu^{2+} + 2e^{-}, \quad (2)$$

for reduction in a solution with Cu^{+}

$$Cu_{x-1}Mo_6S_{7.8} + Cu^{+} + e^{-} \longrightarrow Cu_xMo_6S_{7.8}, \quad (3)$$

and for reduction in a solution with Cu^{2+}

$$Cu_{x-1}Mo_6S_{7.8} + Cu^{2+} + 2e^{-} \longrightarrow Cu_xMo_6S_{7.8}. \quad (4)$$

The redox waves in Fig. 1 correspond to the above reversible intercalations of copper to $Cu_xMo_6S_{7.8}$.

Figure 3 shows a chronopotentiogram of $Cu_3Mo_6S_{7.8}$ under galvanostatic conditions with an oxidation current I=1 mA. This chronopotentiogram shows a positive shift of potential due to deintercalation of Cu^{+}. The Cu composition (x) of the compound decreases with increase in electric quantity (Q) due to oxidative deintercalation. The rest potential of the electrode varies from −0.1 to 0.3 V vs. SCE with oxidation. This electrode potential change which results from stoichiometric variation of $Cu_xMo_6S_{7.8}$ means a shift of the Fermi energy of the compound, which is reflected by variation in electronic distribution within a crystal due to composition change.

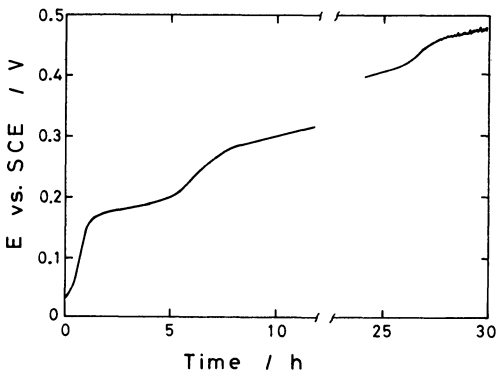

Fig. 3. Chronopotentiogram of a potential of $Cu_3Mo_6S_{7.8}$ under a galvanostatic oxidation with 1 mA in a 0.1 M KNO_3 solution.

It is reported that group compounds with a rhombohedral Chevrel phase contain a variety of metal cation intercalants and that their widely varying superconducting properties depend on both their stoichiometry and crystal structure.[9,10] From the results shown in Figs. 1 and 2, the conformation change of Chevrel phase compounds is expected to be associated with the composition change resulting from the copper cation transfer across the electrode-solution interface. The electric quantity (Q) which is consumed in the course of electrochemical intercalation and deintercalation can affect the stoichiometry of compounds. The relationship between crystal structure of compounds and redox electrolysis was investigated. Powder X-ray diffraction analyses were carried out for compounds $Cu_xMo_6S_{7.8}$ after redox treatment under in galvanostatic conditions with +/− 5 mA. Figure 4 shows the powder X-ray diffraction patterns which were obtained for $Cu_2Mo_6S_{7.8}$ after oxidations with Q=0, 6, and 12 C. The phenomenon that the diffraction patterns change with the degree of oxidation indicates conformation change in crystal. These patterns were analyzed by the Hull-Davey method. Lattice constants for hexagonal unit cell were calculated and converted into those for rhom-

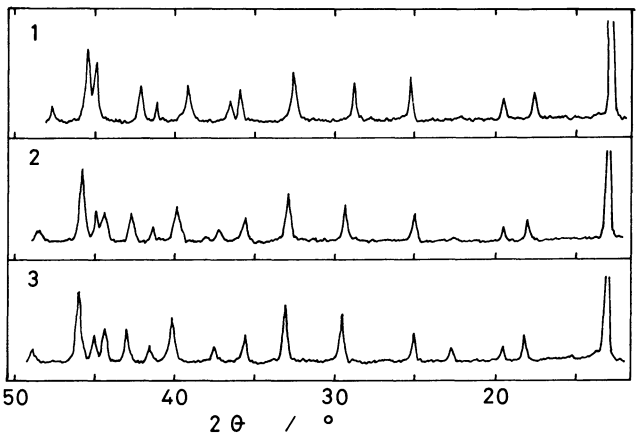

Fig. 4. X-Ray diffraction patterns with Cu $K\alpha$ in the course of an oxidation of $Cu_2Mo_6S_{7.8}$ (0.3 g).
(1) Initial $Cu_2Mo_6S_{7.8}$ (2) oxidized with 6 C, (3) oxidized with 12 C.

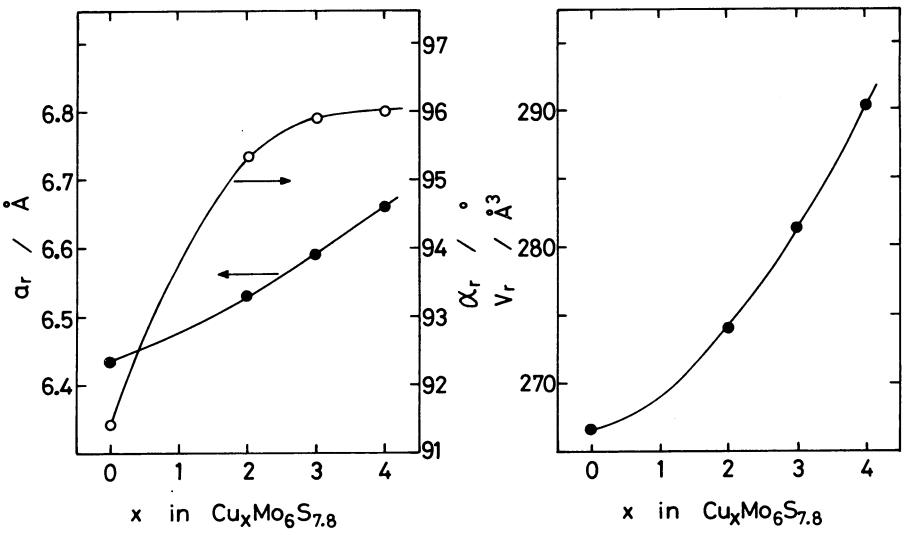

Fig. 5. Lattice constants of $Cu_xMo_6S_{7.8}$ compounds as a function of Cu composition (x).

bohedral unit cell.[16] The rhombohedral crystal structure of $Cu_2Mo_6S_{7.8}$ changes with the electric quantity in oxidation processes.

For the Chevrel phase compounds $Cu_xMo_6S_{7.8}$ (x=0, 2, 3, and 4) which were synthesized with stoichiometric ratios, their rhombohedral structures were also analyzed before redox electrolysis. Figure 5 shows the rhombohedral lattice constants (a_r and α_r) and unit cell volumes (V_r) as a function of Cu composition (x) as determined by the quantitative analysis of dissolved Cu^+ described in the experimental section. This relationship shows a clear dependence of the Chevrel phase structure on Cu composition (x), as described in detail elsewhere.[17] The compounds with various Cu compositions are employed for redox electrolysis, and their structure changes are analyzed as a function of the electric quantity (Q) consumed during the electrolysis.

Figure 6 shows the relationship between rhombohedral lattice constants (a_r, α_r) and oxidative electric quantity (Q_{ox}) for $Cu_4Mo_6S_{7.8}$. Before oxidation, the sample has a rhombohedral structure with a_r=6.65 Å, α_r=96.5°, and V_r=287.5 Å^3. In the course of oxidation, the lattice constants drastically decrease in proportion to the oxidative Q_{ox} to a_r=6.5 Å, α_r=94°, and V_r=273 Å.[3] For $Cu_3Mo_6S_{7.8}$ and $Cu_2Mo_6S_{7.8}$, phenomena similar to that of $Cu_4Mo_6S_{7.8}$ were observed with respect to the relationship between oxidative Q_{ox} and lattice constants, as shown in Figs. 7 and 8. Both a_r and α_r decrease with the degree of oxidation. Especially, the change in lattice angle α_r is characteristic of distorted contraction of crystal. The volume difference (ΔV_r) between $Cu_4Mo_6S_{7.8}$ and $Mo_6S_{7.8}$ is ca. 25 Å^3, which is ca. 10% of the unit cell volume and larger than the ionic volume (14.8 Å^3) as calculated for 4 Cu^+ by using the Cu^+ ionic radius of 0.96 Å.[18] These anisotropic changes in lattice

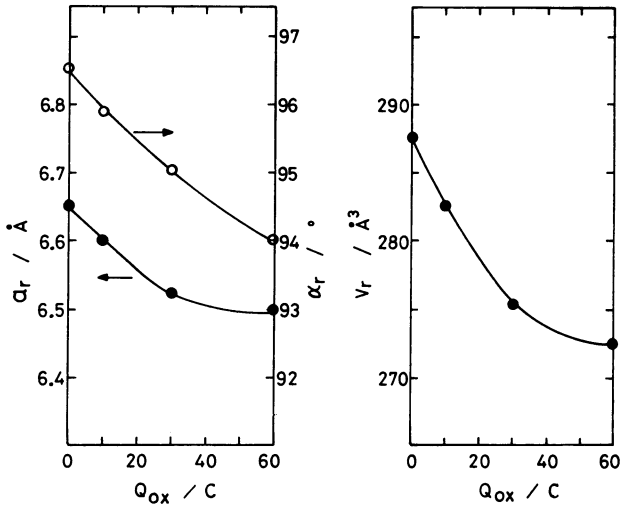

Fig. 6. Dependence of lattice constants on Q_{ox} for an oxidative deintercalation of $Cu_4Mo_6S_{7.8}$.

constants as a function of Q_{ox} claim that the deintercalation process gives rise to a series of changes from $Cu_4Mo_6S_{7.8}$ through $Cu_3Mo_6S_{7.8}$ and $Cu_2Mo_6S_{7.8}$ to the copper-free $Mo_6S_{7.8}$. As seen from a comparison of the crystal parameters in Figs. 6—8 with that in Fig. 5, the copper composition (x) decreases by 1 for each Q_{ox}=ca. 27 C for these compounds:

$$Cu_4Mo_6S_{7.8} \xrightarrow[-e^-]{-Cu^+} Cu_3Mo_6S_{7.8} \xrightarrow[-e^-]{-Cu^+} Cu_2Mo_6S_{7.8} \xrightarrow[-e^-]{-Cu^+} CuMo_6S_{7.8} \xrightarrow[-e^-]{-Cu^+} Mo_6S_{7.8}. \quad (5)$$

When the compound was oxidized at a potential (>0.35 V) in the rane [B], a change in crystal structure similar to that occurring in the range [A] was observed. However, a constant change in lattice

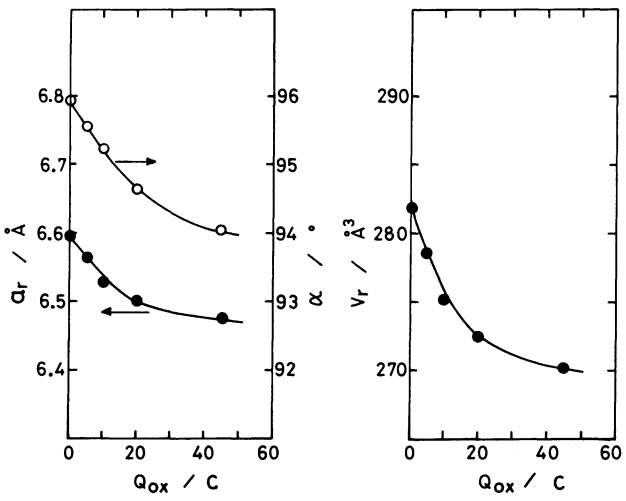

Fig. 7. Dependence of lattice constants on Q_{ox} for an oxidative deintercalation of $Cu_3Mo_6S_{7.8}$.

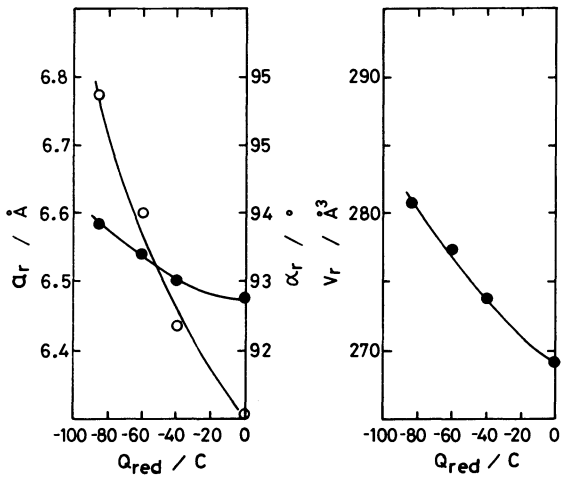

Fig. 9. Dependence of lattice constants on Q_{red} for a reductive intercalation of $Mo_6S_{7.8}$ in a saturated CuCl solution.

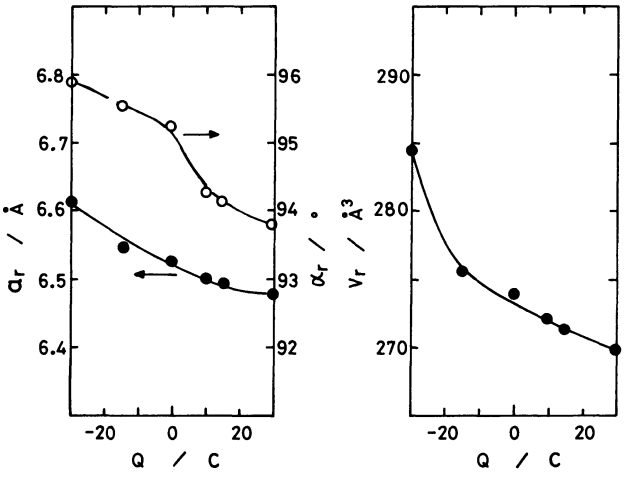

Fig. 8. Dependence of lattice constants on Q for redox intercalation and deintercalation of $Cu_2Mo_6S_{7.8}$.

constant required nearly twice Q_{ox} for the case in the potential range [A]. This means that the deintercalation process according to Eq. 2 involves an oxidation process from Cu^+ to Cu^{2+} at the surface of electrode.

On the other hand, when the sample is reduced, that is, intercalated with Cu^+, it is expected that reverse change in crystal structure will occur in proportion to the reductive electric quantity (Q_{red}), because the cyclic voltammogram of the compound is reversible as shown in Fig. 1. When $Cu_2Mo_6S_{7.8}$ is reduced in a saturated CuCl solution, the crystal structure changes as shown in Fig. 8. In the range of negative Q, the lattice constants increase as intercalation proceeds. Figure 9 shows the relationship between lattice constant and reductive Q_{red} in the course of intercalation for $Mo_6S_{7.8}$. Cu^+ intercalation into a host compound results in increase in the lattice constants, that is, expansion of the crystal unit cell.

When an $Mo_6S_{7.8}$ electrolde was reduced in a solution with 0.1 M Cu^{2+}, similar increases in the lattice constants were observed. However, a certain constant degree of intercalation required nearly twice the Q_{red} for the case with Cu^+, that is, the crystal structure at Q_{red}=40 °C with Cu^+ was almost the same as that at Q_{red}=80 °C with Cu^{2+}. This phenomenon suggests that the intercalation reaction according to Eq. 4 involves a reduction process of Cu^{2+} to Cu^+. This result is consistent with the state of copper(I) cation in crystal disclosed by a crystallographic analysis.[9] Therefore, the intercalation and deintercalation of the compound are transfer processes of copper(I) cation across the compound-solution interface.

As seen from the results of Figs. 6—9, the structures of the rhombohedral crystals undergo reversible and continuous change during the redox intercalation and deintercalation processes of Cu^+. The unit cell of the compound expands due to intercalation and contracts due to deintercalation of Cu^+, accompanying structure distortions due to change in lattice angle.

Figure 10 shows the schematic view of a basic rhombohedral Chevrel phase compound. The copper which is surrounded by the S quasi cubics can be deintercalated by oxidation and intercalated reduction. The crystal deformation results from the effect that the Cu^+ intercalation gives rise to change in the relative distances among the S quasi cubics as well as among the Mo_6 octahedra. Moreover, in the course of the redox processes, if the ionic condition is kept as Cu(+1) and S(2−) in $Cu_xMo_6S_{7.8}$ crystal, the valency Z of Mo shifts from 2.6 to 1.93 due to intercalation. That is, the electron density of a Mo_6 cluster also increases due to intercalation. As electronic structure is generally correlated to crystal structure, the electronic

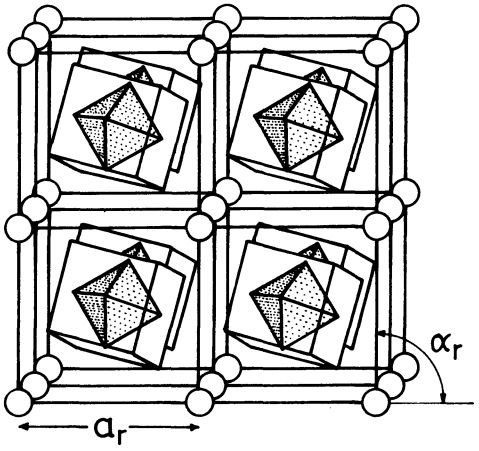

Fig. 10. Schematic illustration of a rhombohedral Chevrel phase compound. Circles denote the Cu Sites. A sulfur cubic contains an octahedral molybdenum Mo_6 cluster.

distribution as well as the density of states of the compound should be affected by the metal cation intercalation and deintercalation. This can explain the observation that the deintercalation of a Cu^+ intercalant from the compound results in a shift of electrode potential which is equivalent to a Fermi energy level, as discussed in connection with the result shown in Fig. 3. The phenomenon that critical temperature T_c of $Cu_xMo_6S_8$ associated with superconducting phenomena varies with Cu composition,[9,10] is evidence for the intercalation effect which leads to change in both the d-electron density of Mo and the crystal structure. Therefore, electrochemical intercalation is useful for studies on superconducting properties of these compounds.

References

1) R. Chevrel, M. S. Sergent, and J. Prigent, *J. Solid State Chem.*, **3**, 515 (1971).
2) J. Hauk, *Mat. Res. Bull.*, **12**, 1015 (1977).
3) R. Flukiger, R. Baillif, and E. Walker, *Mat. Res. Bull.*, **13**, 7443 (1978).
4) S. Yamamoto, K. Matsui, M. Wakihara, and M. Taniguchi, *Mat. Res. Bull.*, **18**, 1311 (1983).
5) R. Chevrel and M. S. Sergent, in "Topics in Current Physics," ed by O. Fischer and M. B. Maple, Springer-Verlag, Berlin (1982), Vol. 32, pp. 25—86.
6) Y. Takeda, R. Kanno, M. Noda, and O. Yamamoto, *Mat. Res. Bull.*, **20**, 771 (1985).
7) R. Chevrel, M. Hirrien, and M. Sergent, *Polyhedron*, **5**, 87 (1986).
8) O. Fischer, *Appl. Phys.*, **16**, 1 (1978).
9) K. Yvon, in "Current Topics in Materials Science," ed by E. Kaldis, Elsevier, Amsterdam (1979), Vol. 3, pp. 53—130.
10) R. Flukiger and R. Baillif, in "Topics in Current Physics," ed by O. Fischer and M. B. Maple, Spriner-Verlag, Berlin (1982), Vol. 32, pp. 113—142.
11) "Physics and Chemistry of Materials with Layered Structures," ed by F. A. Levy, Reide, Dortrecht, (1979), Vol. 6.
12) M. Ikebe and Y. Muto, *Kotai Butsuri*, **16**, 428 (1981).
13) T. Inoue and T. Yamase, *Denki Kagaku*, **54**, 812 (1986).
14) A. Fujishima, M. Aizawa, and T. Inoue, "Denkikagaku Sokuteiho," Gihodo, Tokyo (1984).
15) T. Inoue, T. Watanabe, A. Fujishima, K. Honda, and K. Kohayakawa, *J. Electrochem. Soc.*, **124**, 719 (1977).
16) B. D. Cullity, "Elements of X-Ray Diffraction," Addison-Wesley Pub. Co. Inc., Massachusetts (1956).
17) R. Flukier, R. Baillif, J. Muller, and K. Yvon, *J. Less-Common Met.*, **72**, 193 (1980).
18) "Lange's Handbook of Chemistry," ed by J. A. Dean, McGraw-Hill, New York (1973).